Materials Research Proceedings 41 (2024) 1517-1526 https://doi.org/10.21741/9781644903131-168

Experimental and finite element investigation on the effect of process parameters in incremental forming of polymeric materials

RAGAI Ihab[1,a *], BUFFA Gianluca[2,b], VANDALINI Andrea[2,c] and FRATINI Livan[2,d]

[1]School of Engineering, The Pennsylvania State University, Erie, PA 16563, USA

[2]Department of Engineering, University of Palermo, Viale Delle Scienze, 90128 Palermo, Italy

[a] ihab.ragai@psu.edu, [b] bgianluca.buffa@unipa.it
[c] andrea.vandalini@unipa.it, [d] livan.fratini@unipa.it

Keywords: Incremental Forming, Polymers, Formability, FE Analysis, Isothermal Process

Abstract. The purpose of this paper is to conduct finite element simulations of the incremental forming process of polycarbonate material. The process was simulated using the commercial software LS-Dyna. An explicit loading-implicit unloading approach for springback was set up, reproducing the experimental conditions. The shell element type and the number of integration points along the thickness were defined through a preliminary numerical approach. A spiral 3D surface was generated and measurements of cone geometry were conducted. The model was validated by comparing experimental and numerical thickness in a cross section, and finally used to investigate the effect of step size on the process mechanics. It was found that a decrease in step size would yield to a more uniform thinning along the profile cross section and produces larger thickness reduction.

Introduction

Single-Point Incremental Forming (SPIF) is a merging process that proved to be economical for low-batch production and prototyping purposes. It involves securing the sheet material into a generic fixture, typically a frame-like plate. The forming process takes place by moving a hemispheric tool installed in a CNC machine running a specific code containing the desired geometry. With each pass, the sheet is deformed incrementally, each increment in this process is called the step size. The final shape is achieved by modifying the tool path and the step size. The process is gaining attraction in the forming field due to its low cost, high flexibility, and its capability of forming axisymmetric and asymmetric geometries [1].

There is a significant amount of SPIF-related research conducted on sheet metals [2-7]. However, there is still limited knowledge regarding the use of SPIF with polymeric materials and, therefore, it has been attracting more interest in recent years, due to the nature of failure mechanism, for example [8-11]. Previous research reported that process parameters have significant effect on formability of polymeric materials. Martins et al. [12] conducted research on five different materials, namely polyoxymethylene (POM), polyethylene (PE), polyamide (PA), polyvinyl chloride (PVC), and polycarbonate (PC). Sheets were formed at room temperature, constant spindle speed, and a conical toolpath was utilized. They highlighted the promising possibilities of forming thermoplastic materials. However, they also highlighted the influence of process parameters on formability.

In SPIF, formability can be defined as the maximum wall angle and depth that can be reached prior to failure. In addition to altering process parameters to increase formability, heating the specimens will also enable greater elongation due to the induced thermal softening of the material. Other methods such as tool modification [13,14], vibration-assisted [15,16], and axially-offset rotating tool [17,18] were also reported to increase formability; however, they are not as effective

as heat-assisted forming. Furthermore, it was reported that toolpath modifications and multi-pass will also result in an increase in formability [19,20].

One variable that has been investigated in previous studies is the friction between the tool and the blank and its effect on formability. Bagudanch et al. [21] reported that formability will generally increase due to the increased temperature caused by friction at higher spindle speeds. However, this observation is not necessarily true in all cases. Materials melting and glass-transition temperatures (T_g) played a significant role. When forming temperatures increased, materials with lower melting temperature, such as polypropylene (PP), experienced premature failures; on the other hand, materials with higher T_g, such as PC and PVC, had better formability and experienced a ductile failure. Ragai et al. [1] investigated the effect of tool-workpiece interaction. In their work, they used three different tool materials, namely stainless steel (SS), copper 110 (CU-110), and beryllium-copper (BeCu) as well as three different sheet materials, namely PP, PVC, and PC. They reported that the higher the spindle speed (temperature also increases) the higher the surface roughness of the workpiece, which led to lower formability due to surface deterioration. They also observed that BeCu and Cu-110 tools showed the most promising results in terms of surface condition and formability.

Furthermore, Upcraft et al. [22] conducted a full-factorial 3 × 3 design of experiment test matrix to investigate the effect of feed rate, starting angle, and step size on formability of PP, PVC, and PC materials. It was reported that higher springback would occur with the increase of wall angle. Also, a decrease in wall angle yields a more uniform thinning along the profile cross-section. It was also mentioned that feed rates have no significant effect on material thinning, particularly for 10^o wall angle.

In the study presented herein, the SPIF process of polycarbonate sheets is both experimentally and numerically investigated. The purpose of this work is to examine the possibility of simulating thermoplastic materials undergoing isothermal forming processes. Feed rate and wall angle were kept constant while the step size varied. The FE simulations are validated with the experimental results to determine the models' accuracy and validity.

Materials and Methods

The material tested in the current study is extruded PC sheets. The sheets were received with initial dimensions of 304.8 mm × 304.8 mm [12 in × 12 in] and a nominal thickness of 1.60 mm [0.0625 in], with a tolerance of ±0.076 mm [0.003 in]. Material properties for the sheets are listed in Table 1 [23]. The specimens were then cut to the desired dimensions of 152.4 mm × 152.4 mm and 8 screw holes were drilled along the outer perimeter to help secure the sheets in the fixture.

The forming tool used in this work was BeCu, since it provided better tool-sheet interaction in SPIF, particularly with PC [1]. The geometry of the tool consists of a hemispherical pin with 12.7 mm [0.50 in] diameter and 114 mm [4.50 in] in total length. Table 1 lists the typical mechanical properties for the tool materials [24]. Experiments took place in a HAAS TM 1P CNC milling machine. The square sheets were placed in an aluminum fixture that has a 115 mm [4.5 in] square pocket and provided a work depth of 50 mm [2 in]. Figure 1 shows the experimental setup.

Table 1. Nominal material properties

Material	Yield Strength MPa [psi]	Ultimate Strength MPa [psi]	Elongation [%]	Young's Modulus GPa [ksi]	Shear Modulus MPa [psi]	Rockwell Hardness	Density g/cm^3 [lb/in^3]
PC	62 [9,000]	66 [9,500]	110	2.34 [340]	786 [114,000]	M70/R118	1.19 [0.043]
BeCu	1000 [145]	1170 [170]	5	131 [19,000]	-	C40	8.36 [0.302]

Materials Research Proceedings 41 (2024) 1517-1526 https://doi.org/10.21741/9781644903131-168

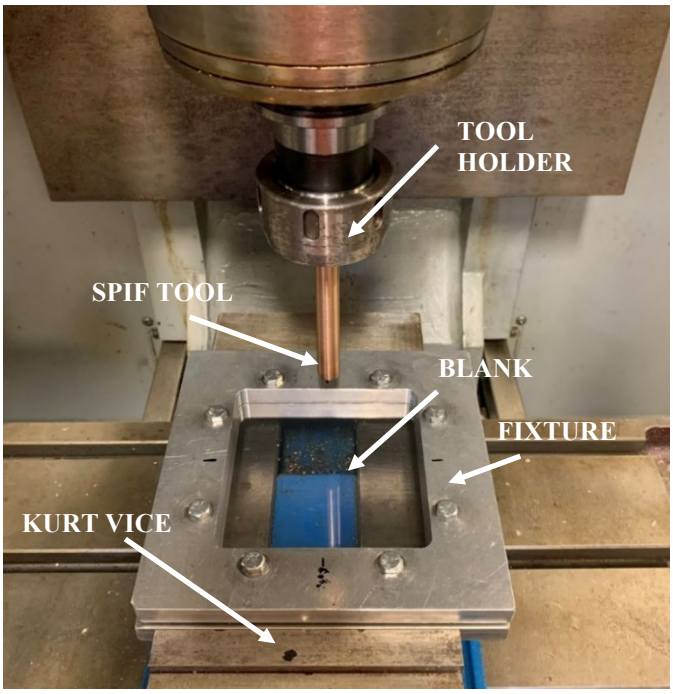

Fig. 1. Experimental setup

The formed part was a cone-shaped geometry that was generated using Mastercam. The theoretical geometry of the formed shape is illustrated in Fig. 2. For the research presented herein, the feed rate was kept constant at 2000 mm/min, the starting angle at 20 degrees, and the step size took values of 0.1, 0.5, and 1.0 mm. The program ran until completion or sample failure.

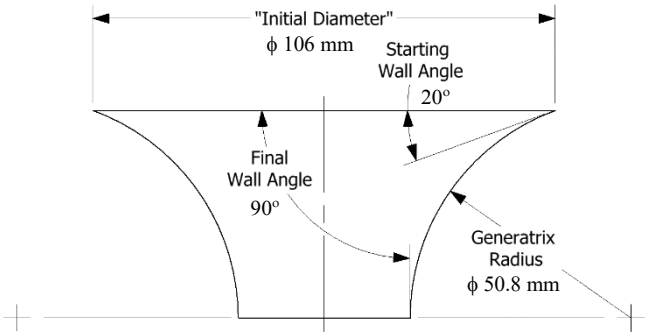

Fig. 2. Cone geometry

After the cones were formed, a Sharpe and Gage 2000 CMM was utilized to measure the profile at 14 points taken across the profile, as shown in Fig. 3. The horizontal (X-) and vertical (Z-) axes of the coordinate machine were free to move while the transverse (Y-) axis of the machine was locked. This ensures accurate measurements along the X-Z plane. These points are then used to represent the formed geometry. Additionally, a Magna-Mike 8600, with a 1.5875 mm [0.0625 in] ball, was utilized to measure the thickness of the profile at the aforementioned datum points.

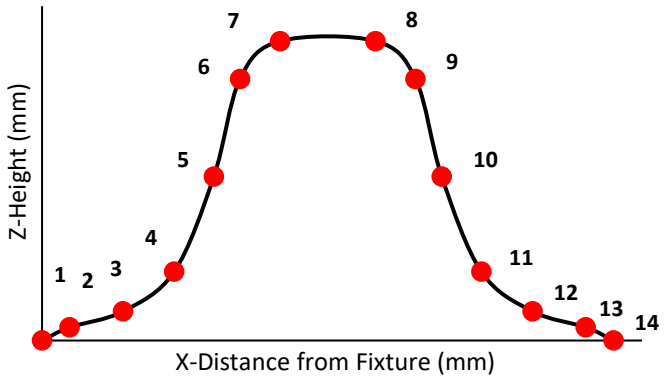

Fig. 3. Profile measurement points

Commercial finite-element-analysis software (ABAQUS/Explicit) was utilized to conduct the numerical simulations. The workpiece was modeled using S4R shell elements with a thickness of 1.6 mm, featuring 5 integration points through the thickness and a mesh size of 1 mm in the tool movement zone. Outside this zone, a coarser mesh characterized by an average size of 2mm was used and a transition zone between the finer and coarser mesh areas was assigned. The tool was treated as a rigid body, and a friction coefficient of 0.05 was set for the interaction between the tool and the workpiece. The experimental fixture effect was modeled by applying encastre boundary conditions to all the nodes at the edge of the fixture. As the tool movement is regarded, this was derived from the G-code used for the experiments and provided, for each process condition, in tabular form. Figure 4 shows the model ready for the simulation.

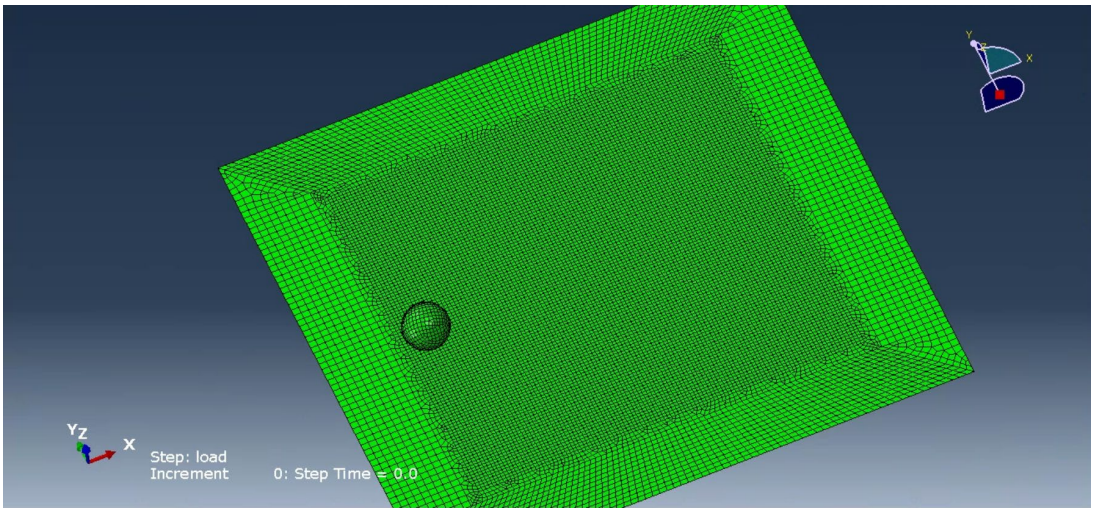

Fig. 4. Numerical model mesh at the beginning of the process

The material's elastic behavior was characterized by a Young's modulus (E) of 2.34 GPa and a Poisson's ratio (ν) of 0.38. Plastic behavior was defined in the form of tabular data according to the information provided by the supplier, as listed in Table 1. For the springback prediction, an implicit analysis was carried out.

Experimental Results

In the current study, the starting angle of 20° is considered a moderate angle compared to a shallow 10° angle, for example. Therefore, the formed geometry produced a U-shaped profile, as opposed to a "V-" shape for smaller angles. Additionally, all experiments ran until program completion as no failures were detected. Springback can be defined as the deviation of the incrementally formed

shape from the desired, theoretical, geometry. Figure 5 shows the profile for each step size with respect to the horizontal, x-position. It is observed that all samples reached an average height of approximately 29 mm. As mentioned earlier, no failure was detected along the walls of the profile. Additionally, it is shown that step size has some minor effect on both formability and shape deviation or springback. For the given values of step sizes (0.1, 0.5, 1.0 mm), it is shown that the decrease in step size will result in a slight increase in formability. This could be attributed to the multiple passes a location would experience in the case of smaller step size. In other words, with a tool diameter of 12.7 mm, a step size of 1.0 mm will not have the same number of overlapping spiral passes as the 0.1 mm step size, it will have less passes. Thus, the material will deform less at these locations. This is also observed in the run time, the 0.1 mm step size required over 2 hours of machine operation versus slightly over 20 minutes for the 1.0 mm step size. Also, springback is observed, as shown by the offset of the profiles in Figure 5. However, it was not possible to experimentally quantify the effect of this process parameter since the overall geometries overlapped or crossed over at certain locations, particularly for the 0.5 mm step size. The offset of the righthand side of the profile could be attributed to the way the sample is mounted in the fixture during measurements and is worth investigating in future studies.

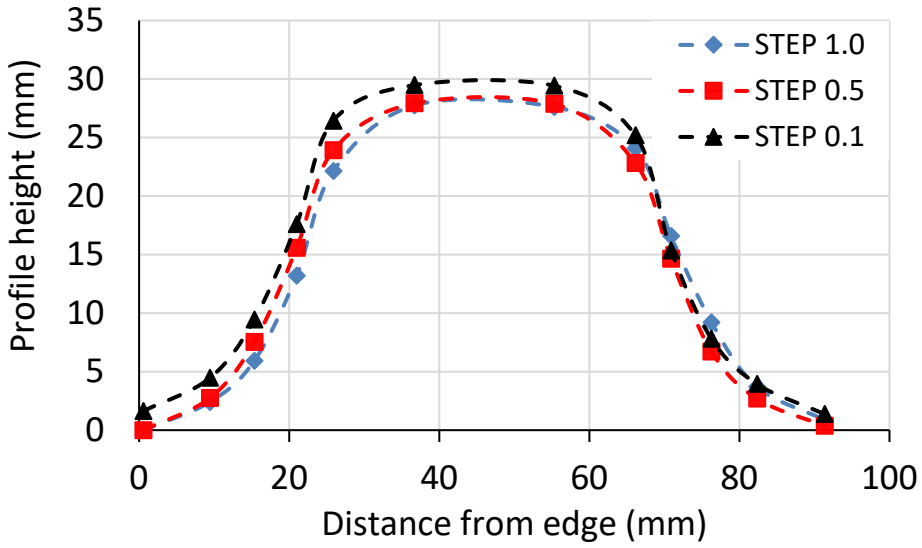

Fig. 5. Shape profiles for incrementally formed PC sheets at different step sizes (Process parameters: feed = 2000 mm/min, wall angle = 20º, spindle = free spin)

Thickness at the datum points was recorded and plotted against the horizontal position, as shown in Figure 6. It is expected that since the decrease in step size results in increased formability, the side walls of the profile would experience uniform thinning as the material stretches. In the smaller step size experiments, the material experiences larger thickness reduction. The purpose of reporting the full profile, rather than only one half for axisymmetry, is to highlight possible slight differences in the profile due to the way the part is fixed. To quantitively capture the amount of thickness reduction along the profile wall, the per cent reduction (compared to 1.6 mm initial thickness) was calculated at the datum points previously presented in Fig. 3. Taking into consideration that the shape is axisymmetric and the differences along the profile can be neglected, Fig. 7 shows that the maximum thickness reduction for all samples is averaged at 52%. It can be generalized that the decrease in step size would result in an increase in thickness reduction of the material. Points (7,8) and (2,13) are at the transition sections and therefore experienced the minimum forming and minimum change in thickness.

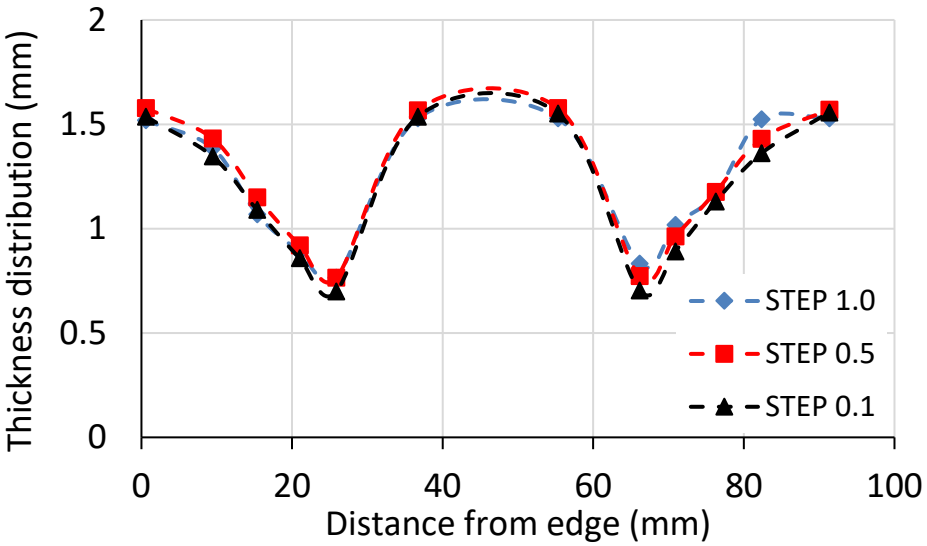

Fig. 6. Thickness distribution for incrementally formed PC sheets at different step sizes (Process parameters: feed = 2000 mm/min, wall angle = 20º, spindle = free spin)

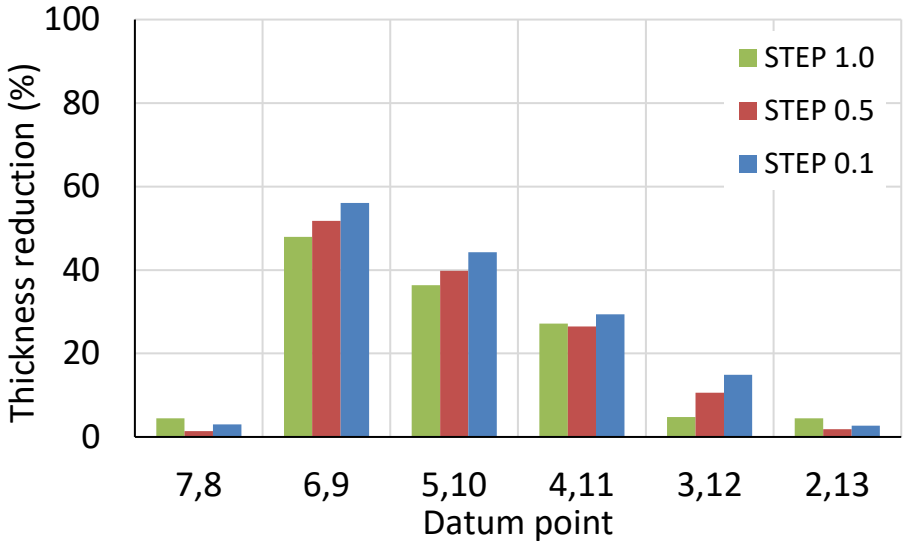

Fig. 7. Thickness reduction % for incrementally formed PC sheets at different step sizes (Process parameters: feed = 2000 mm/min, wall angle = 20º, spindle = free spin)

Simulation Results

First the numerical model was validated against part profile and thickness distribution in a cross section. Figure 8 shows the comparison between measured and calculated data for the case study characterized by step size of 1mm. From the figure, it can be seen that good agreement is obtained for both thickness distribution (Fig. 8a) and profile height (Fig. 8b), although a few discrepancies can be observed especially in profile height. This is due to the springback step simulation which will be fine-tuned (ongoing work) in order to produce more accurate results.

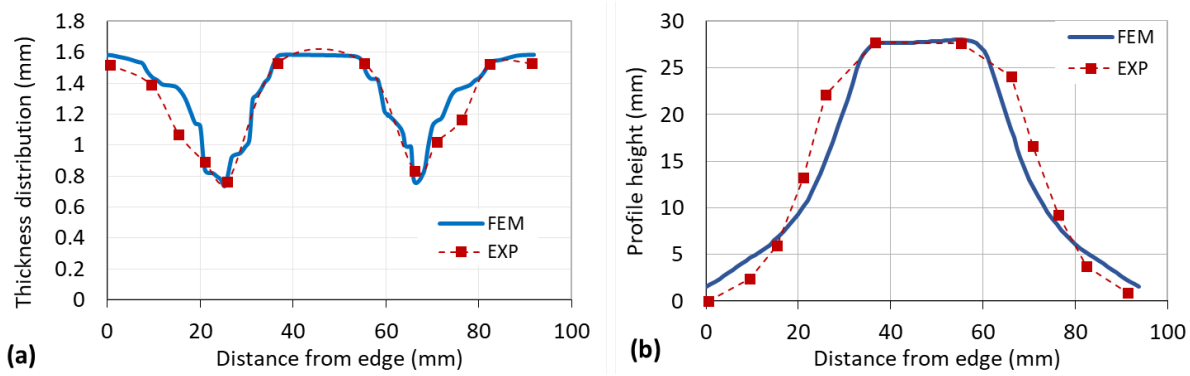

Fig. 8. Comparison of experimental and numerical (a) thickness distribution and (b) profile height for a step size = 1.0 mm

The model was then used to predict the equivalent plastic strain that the material experiences during the process. Figure 9a shows the evolution of the plastic strain during the simulation, while Figure 9b shows the trends of the same variable at the end of the simulation, for the three considered case studies.

Due to the increasing wall angle of the cone geometry, strain increases to a maximum value, corresponding to the fillet area, before dropping to zero at the bottom of the cone. This trend is common for the three step-down values. However, a major difference is found in the peak value in the case of 0.1 mm step size. As experimentally observed, in these process conditions a larger thickness reduction is measured, particularly in the control points closer to the fillet zone, i.e., points 6-9. As to the numerical prediction, similar maximum strain values are calculated for step sizes of 1.0 and 0.5 mm, corresponding to about 2, while a slightly larger value is predicted for the step size of 0.1 mm condition, for which maximum plastic strain reaches a value of about 2.5. For the latter case, the area interested by the larger strain values and the largest difference with respect to the other two cases, corresponds to a distance from the edge ranging from about 25 mm to about 35 mm. This result is in good agreement with the ones shown in Figs. 5 and 7.

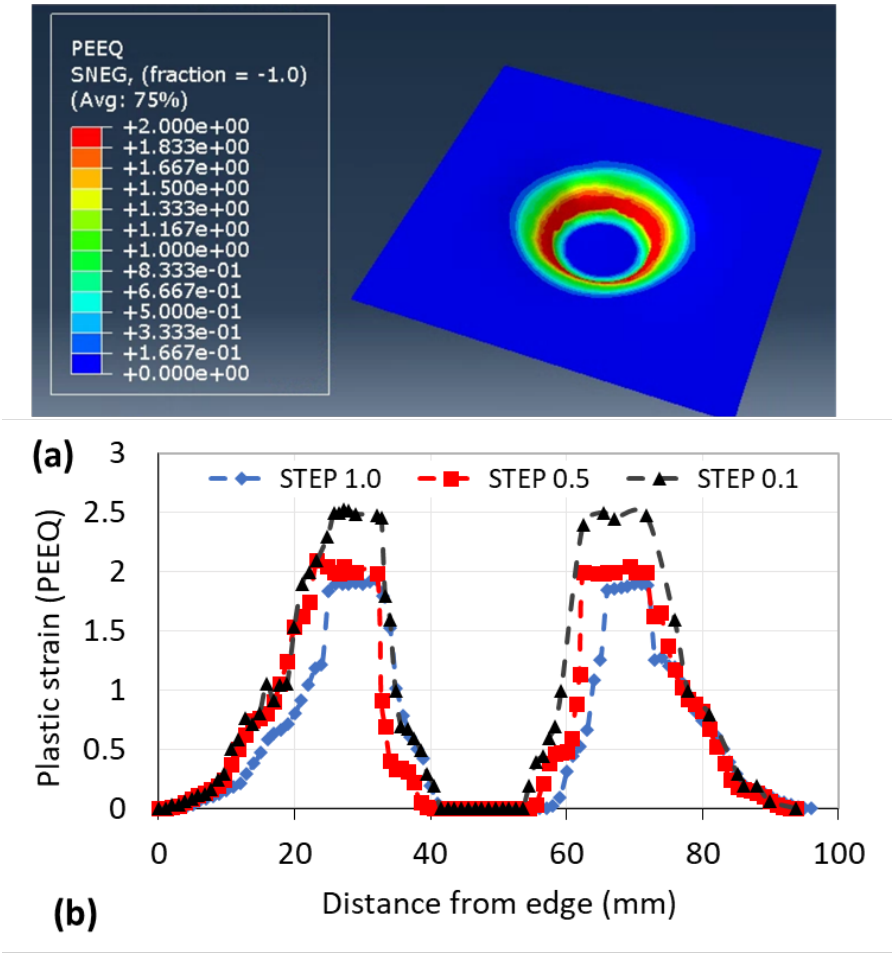

Fig. 9. (a) 3D view of the strain distribution during the forming process and (b) effective plastic strain profiles for the three step size cases

Summary

The work presented in this study highlights the effect of step size in incremental forming of polycarbonate material. Experiments took place where the wall angle of 20º and the feed rate of 2000 mm/min were kept constant throughout the experiments. The spindle of the CNC machine was unlocked and was free to rotate as the forming tool was in contact with the workpiece. Three step sizes were investigated, namely 0.1, 0.5, and 1.0 mm. It was found that the change in step size did not have a significant effect on springback. However, it was generally observed that the smaller step size the more sheet thinning, or thickness reduction, was observed. This was attributed to the multiple passes the material had to go through to achieve the desired height.

Additionally, a commercial finite element code was utilized to simulate the process parameters investigated experimentally. The model was first validated against profile height and thickness distribution, and then used to investigate the effective plastic strain distribution along a cross section of the cone, for the different step size values considered. This analysis highlighted the larger deformation occurring when small step size values are implemented (i.e. 0.1 mm) resulting in a slightly thinner final part.

Future work will focus on extending the investigation to include more process parameters, for example, additional values for the step size as well as various wall angles.

References

[1] I. Ragai, J. Goldstein, C. Meyer, and C. Upcraft, Effect of Tool Material and Process Parameters on Surface Conditions in SPIF of Polymeric Materials, Proc. of the ASME 2022 Int Mech Eng Cong and Expo (2022), Columbus, OH, USA. https://doi.org/10.1115/IMECE2022-95951

[2] G. Palumbo and M. Brandizzi, Experimental investigations on the single point incremental forming of a titanium alloy component combining static heating with high tool rotation speed, Materials & Design, 2012, pp. 43-51. https://doi.org/10.1016/j.matdes.2012.03.031

[3] P. E. Romero, O. Rodriguez-Albanda, E. Molero, and G. Guerrero-Vaca, Use of the Support Vector Machine (SVM) algorithm to predict the geometrical accuracy in the manufacture of molds via single point incremental forming (SPIF) using aluminized steel sheets, Journal of Materials Research and Technology, 2021, pp. 1562-1571. https://doi.org/10.1016/j.jmrt.2021.08.155

[4] M. Milutinović, R. Lendjel, S. Balos, D. L. Zlatanovic, L. Sevsek, and T. Pepelnjak, Characterization of geometrical and physical properties of a stainless-steel denture framework manufactured by single-point incremental forming, Journal of Materials and Research Technology, 2021, pp. 605-623. https://doi.org/10.1016/j.jmrt.2020.12.014

[5] J. Jeswiet, F. Micari, G. Hirt, A. Bramley, J. Duflou, and J. Allwood, Asymmetric single point incremental forming of sheet metal, CIRP Annals, 2005, pp.88-114. https://doi.org/10.1016/S0007-8506(07)60021-3

[6] B. J. Ruszkiewicz, S. S. Dodds, Z. C. Reese, J. T. Roth, and I. Ragai, Incrementally Formed Stiffeners Effect on the Reduction of Springback in 2024-T3 Aluminum after Single Point Incremental Forming, ASME International Manufacturing Science and Engineering Conference (2015), Charlotte, NC, USA. https://doi.org/10.1115/MSEC2015-9437

[7] T. J. Grimm, I. Ragai, and J. T. Roth, Utilization of wavy toolpath in single-point incremental forming, ASME 2018 Int Mech Eng Cong and Expo (2018), Pittsburgh, PA, USA. https://doi.org/10.1115/IMECE2018-86885

[8] H. Zhu, H. Ou, and A. Popov, Incremental sheet forming of thermoplastics: a review, Int J Adv Manuf Technol 111 (2020) 565–587. https://doi.org/10.1007/s00170-020-06056-5

[9] M. A. Davarpanah, and R. Malhotra, Formability and Failure Modes in SPIF of Metal-Polymer Laminates, Proc. Manuf. 26 (2018), 343-348. https://doi.org/10.1016/j.promfg.2018.07.042

[10] V. Franzen, L. Kwiatkowski, J. Neves, P. A. F. Martins, A. E. Tekkaya, On the capability of single point incremental forming for manufacturing polymer sheet parts, Proceedings of the 9th ICTP-International Conference on Technology of Plasticity (2008), Gyeongju, Korea.

[11] V. Franzen, L. Kwiatkowski, P. A. F. Martins, A. E. Tekkaya, Single point incremental forming of PVC, Journal of Materials and Processing Technology, 2009, pp. 462-469. https://doi.org/10.1016/j.jmatprotec.2008.02.013

[12] P. Martins, L. Kwiatkowski, V. Franzen, A. Tekkaya and M. Kleiner, Single point incremental forming of polymers, CIRP Annals, 2009, pp.229-232. https://doi.org/10.1016/j.cirp.2009.03.095

[13] Y. Li, Z. Liu, W.J.T. Daniel, P.A. Meehan, Simulation and experimental observations of effect of different contact interfaces on the incremental sheet forming process. Mater. Manuf. Process. 29 (2014) 121-128. https://doi.org/10.1080/10426914.2013.822977

[14] B. Lu, Y. Fang, D.K. Xu, J. Chen, H. Ou, N.H. Moser, J. Cao, Mechanism investigation of friction-related effects in single point incremental forming using a developed oblique roller-ball tool. Int. J. Mach. Tools Manuf. 85 (2014) 14–29. https://doi.org/10.1016/j.ijmachtools.2014.04.007

[15] M. Vahdati, R. Mahdavinejad, S. Amini, Investigation of the ultrasonic vibration effect in incremental sheet metal forming process. Proc. Inst. Mech. Eng. Part B J. Eng. Manuf. 231 (2017) 971-982. https://doi.org/10.1177/0954405415578579

[16] G.P. Cai, C.W. Xing, Z.H. Jiang, Z.K. Zhang, Sheet Single point vibration incremental forming process simulation and analysis of process parameters. Advanced Materials Research. 430 (2012) 74–78. https://doi.org/10.4028/www.scientific.net/AMR.430-432.74

[17] T.J. Grimm, I. Ragai, J.T. Roth, A Novel Modification to the Incremental Forming Process, Part 1: Multi-directional Tooling. Procedia Manuf. 10 (2017) 510-519. https://doi.org/10.1016/j.promfg.2017.07.035

[18] T.J. Grimm, I. Ragai, J.T. Roth, A Novel Modification to the Incremental Forming Process, Part 2: Validation of the Multidirectional Tooling Method. Procedia Manuf. 10 (2017) 520-530. https://doi.org/10.1016/j.promfg.2017.07.036

[19] D. Young, J. Jeswiet, Wall thickness variations in single-point incremental forming. Proc. Inst. Mech. Eng. Part B J. Eng. Manuf. 2018 (2004) 218, 1453-1459. https://doi.org/10.1243/0954405042418400

[20] Z. Liu, W.J.T. Daniel, Y. Li, S. Liu, P.A. Meehan, Multi-pass deformation design for incremental sheet forming: analytical modeling, finite element analysis and experimental validation. J. Mater. Process. Technol. 214 (2014) 620-634. https://doi.org/10.1016/j.jmatprotec.2013.11.010

[21] I. Bagudanch, G. Centeno, C. Vallellano and M. Garcia-Romeu, Revisiting formability and failure of polymeric sheets deformed by single point Incremental Forming, Polymer and Degradation Stability, (2017) 366-377. https://doi.org/10.1016/j.polymdegradstab.2017.08.021

[22] C. Upcraft, R. Diefenderfer, C. Vanderwiel and I. Ragai, Toward Better Formability of Polymeric Materials in Single Point Incremental Forming: Effect of Process Parameters, Proc. of the ASME 2023 Int Mech Eng Cong and Expo (2023), New Orleans, LA, USA. https://doi.org/10.1115/IMECE2023-112000

[23] https://www.professionalplastics.com/professionalplastics/content/downloads/MakrolonGPV_Specs.pdf

[24] https://materion.com/-/media/files/alloy/datasheets/moldmax/moldmax-hh-alloy-data-sheet.pdf